Fluorescence Sensing

DOI: 10.1002/ange.201403235

Pattern-Based Detection of Toxic Metals in Surface Water with DNA Polyfluorophores**

*Lik Hang Yuen, Raphael M. Franzini, Shenliang Wang, Pete Crisalli, Vijay Singh, Wei Jiang, and Eric T. Kool**

Abstract: *Heavy metal contamination of water can be toxic to humans and wildlife; thus the development of methods to detect this contamination is of high importance. Here we describe the design and application of DNA-based fluorescent chemosensors on microbeads to differentiate eight toxic metal ions in water. We developed and synthesized four fluorescent 2′-deoxyribosides of metal-binding ligands. A tetramer-length oligodeoxy-fluoroside (ODF) library of 6561 members was constructed and screened for sequences responsive to metal ions, of which seven sequences were selected. Statistical analysis of the response patterns showed successful differentiation of the analytes at concentrations as low as 100 nM. Sensors were able to classify water samples from 13 varied sites and quantify metal contamination in unknown specimens. The results demonstrate the practical potential of bead-based ODF chemosensors to analyze heavy metal contamination in water samples by a simple and inexpensive optical method.*

Heavy metal ion pollution is generated through human activities including the use of pesticides and fertilizers, metal plating, and mining operations. The high aqueous solubility of many metal ions allows them to leach into groundwater, increasing the danger of human exposure.[1] In addition to their direct toxicity, heavy metals can cause severe illnesses through bioaccumulation.[2] The World Health Organization estimates that 780 million people (11% of the world population) suffer from drinking unsafe water with toxic metals as major contributors.[3] In the US, 19% of ground water wells exceed metal concentrations allowed by the EPA human health standard.[4] As a result, detecting metal ion contamination is a high priority for protecting human health. Standard laboratory methods such as atomic absorption spectrometry[5] and inductively-coupled plasma mass spectrometry[6] can provide sensitive measurements to identify and quantify metal ions. However, the complexity, expense, and lack of mobility of these methods hinder their application in the field and in developing regions of the world.

Optical detection methods, and in particular optical chemosensor arrays, offer a cost-effective alternative for addressing these limitations. Pattern-based sensing using several colored or fluorescent species enables analysis and differentiation of closely related analyte mixtures even without explicit knowledge of the components. Several examples have demonstrated the potential of optical sensor arrays to detect and analyze biological molecules,[7] environmental contaminants,[8] bacteria[9] and food.[10] Chemosensors for the pattern-based detection of metal ions have also been described.[11] However, the detection limits were generally insufficient to detect metal ions at or below the EPA standards in real-life water specimens.[12]

We have recently described water-soluble fluorescent chemosensors derived from the structure of single-stranded DNA[13] and applied them to the pattern-based analysis of gases,[14] organic vapors[15] and bacteria.[16] In this approach, the natural nucleobases are replaced with fluorescent aromatic groups, enabling sequence-dependent interactions between the fluorophores[17] and yielding specific emission responses to analytes. Such "oligodeoxy-fluoroside" (ODF) molecules can be easily assembled in libraries with thousands of sequences using automated DNA synthesis cycles; using libraries of ODFs, one can rapidly screen for potential sensors with the desired fluorescence responses.

In an early study, we employed dissolved ODFs to differentiate eight metals at 10 μM in buffered background.[18] Those proof-of-principle compounds lacked the sensitivity to detect toxic metals ions below EPA standards (Table S1 in the Supporting Information) and were not tested with real-life water samples. To enhance the applicability of our ODF sensors, we describe here improved molecular chemosensor designs, now on a bead-based platform, and apply them to differentiating EPA-defined toxic metals as contaminants in both pure water and California surface waters.

We designed and synthesized four new deoxyribonucleoside monomers (BC, BP, HQ and QB, Figure 1 A) based on the following criteria: the ability to bind metals with varied selectivities, report ion coordination by fluorescence responses, and remain stable in the presence of metal ions. The quinoline-benzoxazole (QB) monomer was reminiscent of a previous 2,2′-quinolinebenzimidazole ligand nucleoside, which fluorescently responded to several metal ions.[19] The C–N glycosidic bond of that ligand-nucleoside had a tendency to lability, whereas QB is a stable C-nucleoside. The 8-hydroxyquinoline (HQ) monomer was based on a recently described chemosensor compound that emits green fluorescence upon metal binding.[20] The BP monomer contains a 2,2′-bipyridine structure—a widely used ligand in coordi-

[*] L. H. Yuen,[+] Dr. R. M. Franzini,[+] Dr. S. Wang, Dr. P. Crisalli, Dr. V. Singh, Dr. W. Jiang, Prof. Dr. E. T. Kool
Department of Chemistry, Stanford University
Stanford, CA 94305 (USA)
E-mail: kool@stanford.edu

[+] These authors contributed equally to this work.

[**] We thank Eni S.p.A. and the U.S. National Institutes of Health (GM067201) for support.

Supporting information for this article is available on the WWW under http://dx.doi.org/10.1002/anie.201403235.

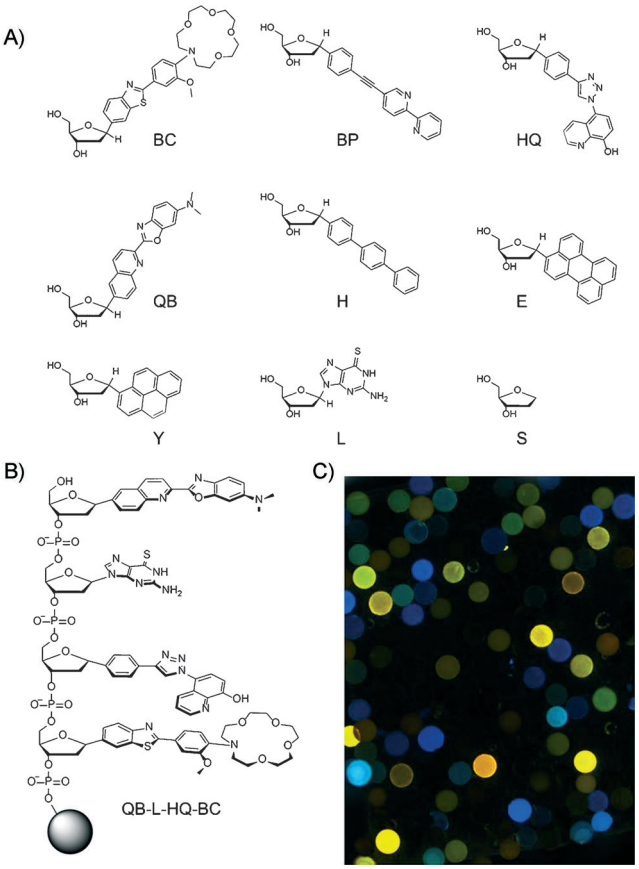

Figure 1. Oligodeoxyfluorosides (ODFs) used for toxic metal ion detection. A) Monomers used in ODF library. BC, BP, HQ and QB were designed and synthesized as new ligands for this study. B) Representative structure of an ODF sensor sequence (QB-L-HQ-BC) on a bead. C) Sample image of ODF library on 130 μm PEG-PS beads, taken by epifluorescence microscope (λ_{ex} = 340–380 nm; λ_{em} > 420 nm)

nation chemistry—with a phenylalkynyl substituent at the C-4 position, to render the ligand fluorescent.[21] The design of BC (an aza-15-crown-5-containing 2-phenylbenzathiazole ligand) was inspired by the molecular sensors developed by Tsien.[22] In addition to the crown-ether moiety, this ligand can likely coordinate metal ions at the benzothiazole nitrogen. Synthesis and characterization details of the four monomers are given in the Supporting Information.

Photophysical properties of the new monomers were measured (Figure S1 and Table 1). The emission bands of the fluorophores were well separated and the maxima ranged from 386 nm to 565 nm. The fluorescence quantum yields and the extinction coefficients of BC, BP and QB were high, with the exception of HQ ($\Phi = 0.005$, $\varepsilon(317\text{ nm}) = 5400\ \text{cm}^{-1}\text{M}^{-1}$; Table 1), which is a fluorescence turn-on sensor.

The four novel ligand monomers and five previously described monomers (Figure 1 A) were derivatized as DMT-protected phosphoramidites to allow library assembly via automated DNA synthesis. Aromatic hydrocarbon fluorophores (E and Y) were incorporated as fluorescence modulators, and non-fluorescent spacers (L, H, and S) were included to diversify the electronic and structural interactions in the ODFs.[18] We assembled a tetrameric ODF library with 6561 distinct monomer sequences (named using letters of each monomer from 5′→3′) on PEGylated polystyrene (PEG-PS) beads using standard split-and-pool methodology (Figure 1 B).[17a,24] Figure 1 C shows a fluorescence image of a subset of the library, revealing a broad range of emission wavelengths and brightness.

Table 1: Photophysical properties of the new 2′-deoxyribo-fluorosides in MeOH.

Deoxyribo-fluoroside[a]	λ_{abs} [nm]	λ_{em} [nm]	ε [$\text{M}^{-1}\text{cm}^{-1}$]	Φ[b] (excitation)	τ [ns]
QB	400	565	21100	0.17 (370 nm)	1.86 ± 0.01
BP	318	386	39900	0.26 (358.8 nm)	0.96 ± 0.01
HQ	271, 317	420	5400	0.005 (331.7 nm)	nd[c]
BC	364	447	27400	0.17 (358.8 nm)	2.94 ± 0.02

[a] Monomers were present as 3′,5′-diols. [b] Quantum yields were measured at 24 °C referenced to 9,10-diphenylanthracene in EtOH.[23] [c] Could not be measured accurately because of low emission signal.

As analytes we chose eight metal species, Cd^{II}, Cr^{VI}, Cr^{III}, Fe^{III}, Hg^{II}, $MeHg^{II}$, Mn^{II}, and Ni^{II}, which the EPA has defined as drinking water contaminants.[25] (Note that Cr^{VI} exists as CrO_4^{2-} in aqueous solution.)[26] Library screening was performed by taking fluorescence images before and after 1 h incubation of the ODF library in buffered metal ion solution; the two images were digitally compared and beads that showed a difference were isolated and sequenced. 40 strongly-responding candidate sequences, exhibiting a variety of color and brightness, were identified for the eight metals (Table S2). We resynthesized and characterized seven sequences with varied compositions and responses on both non-cleavable PEG-PS beads and cleavable controlled pore glass (CPG). The ODFs on CPG were deprotected, cleaved, purified by HPLC and characterized by MALDI-TOF mass spectrometry to confirm chemical identity (Table S3). The simultaneously-prepared ODFs on beads were subsequently used in chemosensing experiments.

To evaluate the ability of the selected ODF chemosensors to differentiate the toxic metals, we performed a full cross-screening between the seven sensors and 1 μM of each analyte, evaluating 56 combinations (each reproduced on five separate beads). Although significant responses were observed in most cases within 3 h, we discovered that prolonged incubation of the beads in metal ion solution enhanced the signal and improved reproducibility. Beads were thus incubated for 24 h throughout this study (Figure S2). The before/after images were overlaid and digitally subtracted to reveal the fluorescence changes as RGB values.

Our results confirmed the importance of both the monomers and the sequence in ODF sensing. For example, BC-QB-H-H (listed 5′→3′) showed a strong quenching response with $MeHg^{II}$, yet sequences sharing some of the same monomers, (e. g. QB-L-HQ-BC), responded weakly (Figure 2 A). This suggests that the fluorescence changes of the chemosensors depend on cooperative interactions within an oligomer rather than only the additive responses of the individual monomers. Wavelength-selective quenching responses were prevalent,

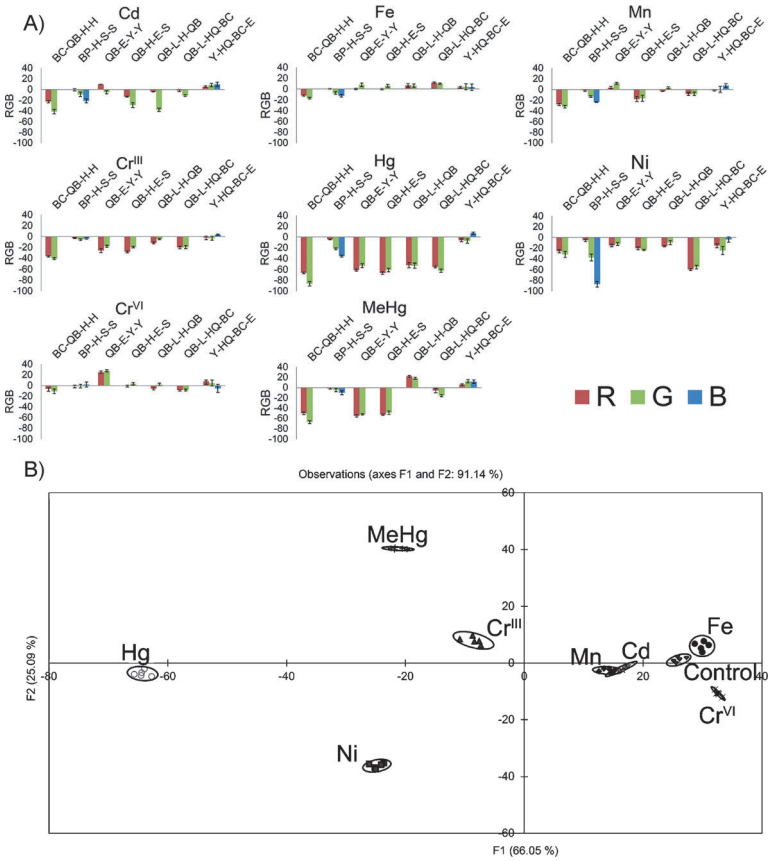

Figure 2. Responses of seven selected chemosensors to metals in buffered deionized water. A) Quantitative fluorescence responses of all sensors toward 8 metals at 1 μM after subtraction of the buffer signal. Red, green and blue bars represent the change in R, G and B channels (on a scale of ±255). The error bars represent one standard deviation from five measurements. B) Results from discriminant analysis of 5 bead responses for each metal projected on the first two principal axes; ellipses indicate 95% confidence level.

with a few lighting-up responses also being observed. The magnitude of the fluorescence response varied for the metals: Hg^{II} and Ni^{II} had strong effects whereas Fe^{III} and Cr^{VI} showed small fluorescence changes with several of the sensors; however, some clear differences can be observed (particularly for sequence QB-E-Y-Y), allowing discrimination by pattern analysis.

To determine the statistical significance of the fluorescence responses to varied metals, we employed discriminant analysis and agglomerative hierarchical clustering (AHC). Discriminant analysis allows visualization of patterns in multi-dimensional data by projecting and categorizing the data into a smaller number of dimensions (principal components) having maximal orthogonality. Figure 2B shows a 2-D projection plot of the discriminant analysis based on the variability of the response from RGB values of all sensor sequences. This 2-D discriminant analysis plot includes 91.1% of the variance and additional orthogonal dimensions enhanced separation further (Figure S3A). Yet the two dimensions alone are sufficient to separate the eight metals shown by the 95% confidence ellipses with the exception of some overlap between Cd^{II} and Mn^{II}.

AHC analysis uses all the data variance and groups the metal responses by similarity into families (see dendrogram in Figure S3B). The cluster analysis successfully categorized all experimental trials for a given metal into the same group while separating the distinct metals into different categories. This demonstrates the ability of these seven ODFs to reproducibly differentiate metal ions at 1 μM concentrations in a pure water/buffer background.

The sensitivity of ODFs to detect metal ions was examined by lowering the analyte concentration to 100 nM. As expected, the dissimilarity between responses from each metal declined with decreasing concentration. With the first two dimensions of discriminant analysis projecting 77.5% of the data variance, a simple 2-D plot incompletely distinguished the metal ions and only $MeHg^{II}$ remained well separated (Figure S4). However, AHC analysis, using all the variance from the data, showed complete differentiation of all metals (Figure 3), further demonstrating the discriminating power of the selected chemosensors even at low concentrations.

To test the potential of ODFs to detect metal ions in surface water, we studied sensor responses to 2 μM metal ion solutions added as contaminants to water from the Merced River (Yosemite National Park, California). This analysis evaluated the effect of realistic levels of background mineral salts (and dissolved organics) on the responses of the chemosensors. Independent analysis of the uncontaminated water sample revealed elevated concentrations of Na^+, and low amounts of the analyte toxic metals (see Table S4).

A full cross-screening was performed between the eight analytes and seven sensor sequences (Figure S5). The buffered stream water alone showed fluorescence responses (Table S5), reflecting dissolved components in the stream water. However, despite the higher background, the presence of metal ions in stream water elicited fluorescence changes similar to those seen in deionized water. Discriminant analysis and AHC revealed the discriminating power of the set of ODFs. All metals showed good separation with little or no overlapping of the 95% confidence ellipses. Again in a 2-D plot of discriminant analysis (Figure 4), fluorescence responses of Fe^{III} were weak and could not be distinguished from the background. However, in the AHC analysis, complete separation of all metal ions was observed (Figure S6).

We further studied the ability of the ODFs to differentiate the eight analytes in stream water at 500 nM and 100 nM ion solutions. Discriminant analysis reproducibly distinguished Cd^{II}, Mn^{II}, $MeHg^{II}$ and Ni^{II} at 500 nM and Ni^{II} and $MeHg^{II}$ at 100 nM from other metals even with the strong background from the surface water (Figure S7). AHC was also performed using the ΔRGB data obtained at the two concentrations and similar results were obtained (Figure S8).

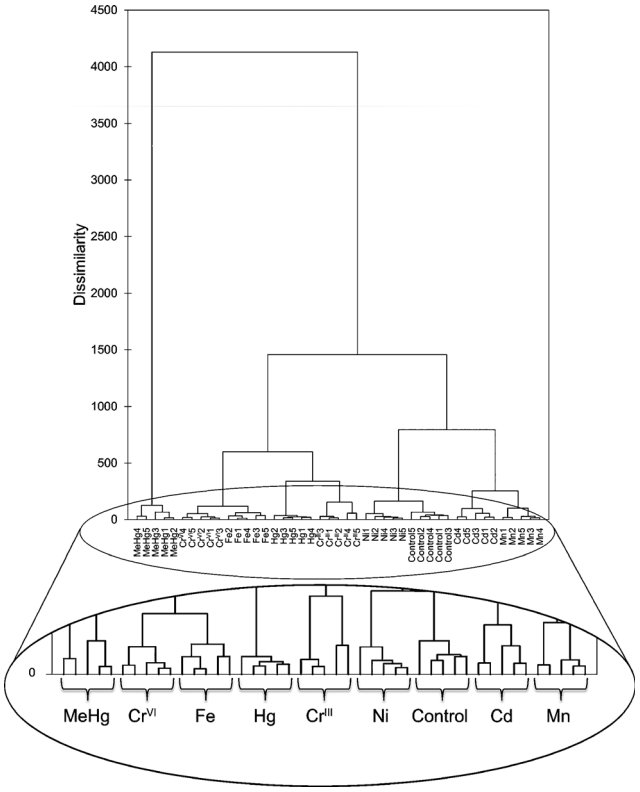

Figure 3. Agglomerative hierarchical clustering (AHC) analysis from 8 metals at 100 nM using 7 ODF sensors in buffered deionized water. All repetitions were grouped together, showing complete discrimination.

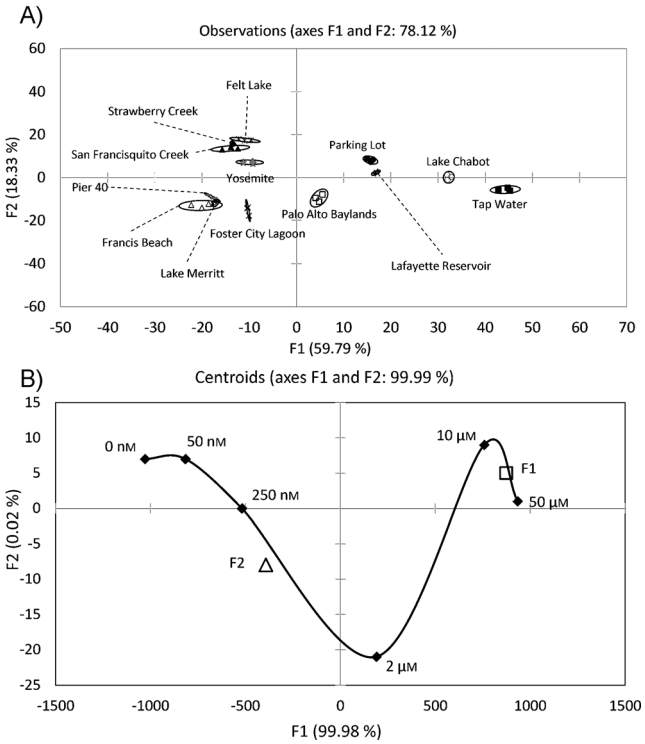

Figure 5. Discriminant analysis of ODF sensors in A) 13 water samples at 2 h incubation and B) Foster City Lagoon water with various concentration of Ni^{II}. The concentrations tested are noted on the figure. F1 (38 µM) and F2 (640 nM) represent the data obtained from blind unknowns.

To further explore practical application, we used the 8 ODF set to classify and discriminate 13 California water samples having varied metal salt compositions and dissolved organics (Figure 5, Table S6). We shortened incubation time to 2 h to make the test more convenient. The AHC dendrogram (Figure S9) clearly separated and clustered the salt water and the fresh water samples, and provided useful information. For example, an Oakland body of water (Merritt) is named as a "lake", but our data show that it is in fact salt water with content similar to a bay sample. A satellite image reveals that it is connected to San Francisco Bay via an open inlet. Among fresh water samples, two local creeks are found to be very similar to one another in content, and two local reservoirs group closely with local tap water (see Figure 5A and further analysis in Figure S9).

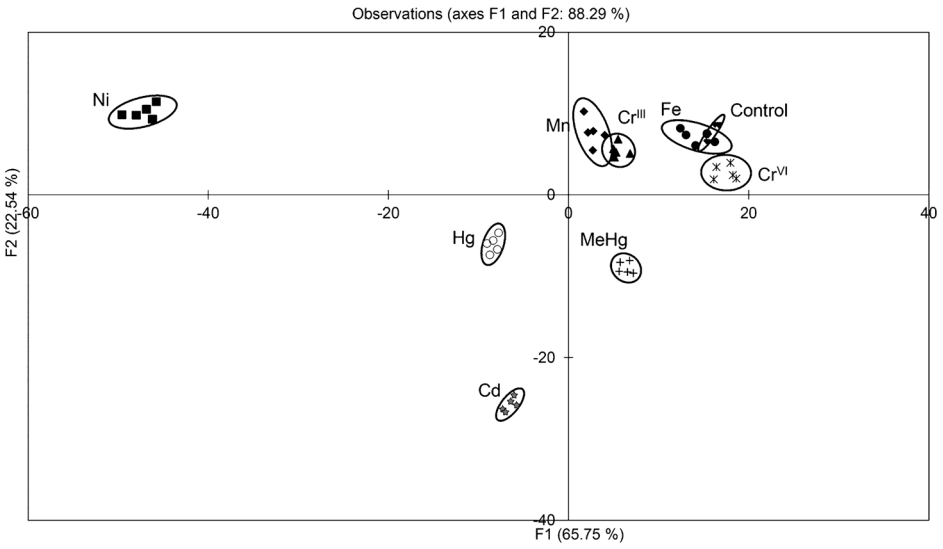

Figure 4. Discriminant analysis of ODF sensors' responses to 8 toxic metals at 2 µM in buffered Yosemite stream water. Results of 5 bead responses for each metal projected on the first two principal axes; ellipses indicate 95% confidence level.

Next we tested the ability of the ODF set to quantify contaminants in the background of natural water. We selected one salt water (Foster City Lagoon) and one fresh water (Lake Chabot) sample and plotted calibration curves using the ΔRGB values from the ODFs at varied concentrations of Ni^{II}. Figure 5B shows the concentration curve plotted with the centroids of triplicate data from DA obtained using the water from Foster City Lagoon (see Figure S11 for Lake Chabot data). The concentration curves show that the ODFs dynamically respond to Ni^{II} at the range 50 µM to 250 nM and the changes diminish below 250 nM, implying that

quantification will be most accurate between 50 μM to 250 nM. To test a practical application, we prepared four unknown samples with varied Ni^{II} contaminants, and plotted them alongside the concentration curves to estimate the concentrations of the unknowns (F1 and F2 in Figure 5B; see also Figure S10). In three of four samples, the unknowns were quantified by interpolation with good accuracy, while the fourth (a 100 nM sample) was underestimated at ca. 40 nM.

In summary, we have developed four novel deoxyribonucleoside monomers that contain ligands with sensitive optical responsiveness to transition metal ions. Although multiple nucleoside derivatives containing either metal ligands or fluorophores have been described, few examples are known that contain both properties.[19,27] Tetrameric DNA-like chemosensors containing these structurally varied ligands provided diverse responses to different metal ions. In particular, such ODFs on beads can readily differentiate between eight toxic metal ions in aqueous solution at 100 nM; five of these metal concentrations were at or below the EPA-defined maximum allowed concentrations (Table S1). The ODF sensors successfully detected eight metal ions in the presence of real-life salt background at 2 μM and two—Ni^{II} and $MeHg^{II}$—at 100 nM. Further, they were able to classify several real-life water samples and quantify concentrations of Ni^{II} contamination in real water backgrounds.

The current approach shows excellent performance when compared to other pattern-based metal sensing methods.[28] ODF sensors demonstrate advantages including excellent sensitivity in water without cosolvents, and extraordinary signal diversities. The sensors on beads are potentially highly mobile and require very little material (less than 1 pmol per measurement); the analysis in principle only requires fluorescence imaging using a simple light source (such as an LED) and readily available image-processing software, hence lowering the cost and time of the analysis. Building sensors on solid support also enhances the ease of chemosensor preparation. With automated DNA synthesis, the ODF sensor assembly proceeds in high yield without the need for purification.

In order to apply ODFs more generally as metal ion sensors, a number of questions remain to be addressed. Testing combinations of toxic metals will be of relevance, since some of the sources of contamination produce multiple heavy metals together. In addition, exploring a larger set of analytes including additional EPA-regulated metals will also be of interest.

Received: March 12, 2014
Published online: April 22, 2014

Keywords: combinatorial chemistry · fluorescence · oligonucleotides · sensors · transition metals

[1] J. O. Nriagu, *Science* **1996**, *272*, 223.
[2] a) C. C. Bridges, R. K. Zalups, *Toxicol. Appl. Pharmacol.* **2005**, *204*, 274; b) L. Järup, *Br. Med. Bull.* **2003**, *68*, 167; c) D. R. Baldwin, W. J. Marshall, *Ann. Clin. Biochem.* **1999**, *36*, 267; d) J. P. Buchet et al., *Lancet* **1990**, *336*, 699 (see Supporting Information).
[3] UNICEF, World Health Organization, *Progress on Drinking-Water and Sanitation: 2012 Update*, New York, Geneva, **2012**.
[4] J. D. Ayotte, J. M. Gronberg, L. E. Apodaca, *Trace Elements and Radon in Groundwater Across the United States, 1992–2003*, U.S. Geological Survey, Reston, Virginia, **2011**, p. 36.
[5] P. Pohl, *TRAC Trends Anal. Chem.* **2009**, *28*, 117.
[6] D. Karunasagar, J. Arunachalam, *Anal. Chim. Acta* **2001**, *441*, 291.
[7] a) O. R. Miranda, C.-C. You, R. Phillips, I.-B. Kim, P. S. Ghosh, U. H. F. Bunz, V. M. Rotello, *J. Am. Chem. Soc.* **2007**, *129*, 9856; b) D. Margulies, A. D. Hamilton, *Angew. Chem.* **2009**, *121*, 1803; *Angew. Chem. Int. Ed.* **2009**, *48*, 1771; c) R. B. C. Jagt, R. F. Gómez-Biagi, M. Nitz, *Angew. Chem.* **2009**, *121*, 2029; *Angew. Chem. Int. Ed.* **2009**, *48*, 1995.
[8] H. Lin, M. Jang, K. S. Suslick, *J. Am. Chem. Soc.* **2011**, *133*, 16786.
[9] A. Bajaj, O. R. Miranda, R. Phillips, I.-B. Kim, D. J. Jerry, U. H. F. Bunz, V. M. Rotello, *J. Am. Chem. Soc.* **2010**, *132*, 1018.
[10] a) C. Zhang, K. S. Suslick, *J. Agric. Food Chem.* **2007**, *55*, 237; b) H. Kwon, F. Samain, E. T. Kool, *Chem. Sci.* **2012**, *3*, 2542.
[11] a) H. S. Hewage, E. V. Anslyn, *J. Am. Chem. Soc.* **2009**, *131*, 13099; b) T. Mayr, C. Igel, G. Liebsch, I. Klimant, O. S. Wolfbeis, *Anal. Chem.* **2003**, *75*, 4389.
[12] a) J.-S. Lee, J. W. Lee, Y.-T. Chang, *J. Comb. Chem.* **2007**, *9*, 926; b) M. A. Palacios, Z. Wang, V. A. Montes, G. V. Zyryanov, P. Anzenbacher, Jr., *J. Am. Chem. Soc.* **2008**, *130*, 10307; c) L.-Y. Niu, H. Li, L. Feng, Y.-S. Y.-F. Guan, Y.-Z. Chen, C.-F. Duan, L.-Z. Wu, C.-H. Tung, Q.-Z. Yang, *Anal. Chim. Acta* **2013**, *775*, 93.
[13] C. Strässler, N. Davis, E. Kool, *Helv. Chim. Acta* **1999**, *82*, 2160.
[14] C.-K. Koo, F. Samain, N. Dai, E. T. Kool, *Chem. Sci.* **2011**, *2*, 1910.
[15] a) W. Jiang, S. Wang, L. H. Yuen, H. Kwon, T. Ono, E. T. Kool, *Chem. Sci.* **2013**, *4*, 3184; b) F. Samain, S. Ghosh, Y. N. Teo, E. T. Kool, *Angew. Chem.* **2010**, *122*, 7179; *Angew. Chem. Int. Ed.* **2010**, *49*, 7025.
[16] C.-K. Koo, S. Wang, R. L. Gaur, F. Samain, N. Banaei, E. T. Kool, *Chem. Commun.* **2011**, *47*, 11435.
[17] a) J. Gao, C. Strässler, D. Tahmassebi, E. T. Kool, *J. Am. Chem. Soc.* **2002**, *124*, 11590; b) Y. N. Teo, J. N. Wilson, E. T. Kool, *J. Am. Chem. Soc.* **2009**, *131*, 3923.
[18] S. S. Tan, S. J. Kim, E. T. Kool, *J. Am. Chem. Soc.* **2011**, *133*, 2664.
[19] S. J. Kim, E. T. Kool, *J. Am. Chem. Soc.* **2006**, *128*, 6164.
[20] J. A. González-Vera, E. Luković, B. Imperiali, *J. Org. Chem.* **2009**, *74*, 7309.
[21] L. Zhang, L. Zhu, *J. Org. Chem.* **2008**, *73*, 8321.
[22] A. Minta, R. Y. Tsien, *J. Biol. Chem.* **1989**, *264*, 19449.
[23] J. V. Morris, M. A. Mahaney, J. R. Huber, *J. Phys. Chem.* **1976**, *80*, 969.
[24] H. P. Nestler, P. A. Bartlett, W. C. Still, *J. Org. Chem.* **1994**, *59*, 4723.
[25] EPA, "National recommended water quality criteria," can be found under http://water.epa.gov/scitech/swguidance/standards/criteria/current/index.cfm, **1998**.
[26] J. McLean, T. J. Beveridge, *Appl. Environ. Microbiol.* **2001**, *67*, 1076.
[27] H. Morales-Rojas, E. T. Kool, *Org. Lett.* **2002**, *4*, 4377.
[28] a) B. García-Acosta, R. Martínez-Mañez, F. Sancenón, J. Soto, K. Rurack, M. Spieles, E. García-Breijo, L. Gil, *Inorg. Chem.* **2007**, *46*, 3123; b) F. Szurdoki, D. Ren, D. R. Walt, *Anal. Chem.* **2000**, *72*, 5250; c) T. Carofiglio, C. Fregonese, G. J. Mohr, F. Rastrelli, U. Tonellato, *Tetrahedron* **2006**, *62*, 1502; d) T. Mayr, G. Liebsch, I. Klimant, O. S. Wolfbeis, *Analyst* **2002**, *127*, 201.

